JOURNAL OF APPLIED ELECTROCHEMISTRY 23 (1993) 190–196

Electrochemical and reflectance study of the conversion of zinc oxide by hexacyanoferrate (II) in offset lithography

Part III: Zinc electrochemistry in hexacyanoferrate (II) and minor components

D. R. ROSSEINSKY, J. D. SLOCOMBE, A. M. SOUTAR

Department of Chemistry, The University, Exeter EX4 4QD, Great Britain

Received 24 July 1992; revised 28 September 1992

Zinc taken from -1.4 to -0.7 V/SCE in the presence of hexacyanoferrate(II) solution generates first a tough glassy material from -1.25 to -1.0 V, breaches through which then produce a gel. The two types of zinc hexacyanoferrate(II) product are probably related to their Zn^{II} oxide and Zn^{2+} (aquo) progenitors. The electrochemistry depends on the zinc pretreatment which governs the amount (from zero, to appreciable) of nucleating Zn^{II} oxide initially present. $H_2PO_4^-$ is shown to play a crucially modifying part, while Na_2EDTA, malic acid, disodium 1-ethoxy-sulphosuccinate surfactant and isopropanol have minor roles in product modification. Possibly procrustean compositions for glass, gel and conversion product are suggested. Diffuse reflectance, AAS, SEM, XRD and i.r. spectroscopy were used in characterisations. The mechanism of electrophotographic conversion is discussed.

1. Introduction

The 'conversion' of zinc oxide in image-free areas to a bulky hexacyanoferrate (II)-containing material, essential to an electrophotographic lithography printing process, has been preliminarily studied [1,2] in Parts I and II by generating Zn^{II} oxide (our abbreviation for the 7 forms of oxide/hydroxide[1]) on a zinc electrode, and observing the electrochemical and visible consequences of adding conversion solution components, so far without hexacyanoferrate (II). The main accompaniment to hexacyanoferrate (II) in the technical solution is NaH_2PO_4, and Part II established its clear but marginal role in electrode processes. Here the effect of the presence of $Na_4Fe(CN)_6$, with and without $H_2PO_4^-$, and of seriatim additions of the remaining minor constituents, are studied.

In the initial stages a novel diffuse reflectance monitor helped clarify the point of appearance of new products, in the 'forward' limbs (-1.4 to -1 V or sometimes -0.7 V) of cyclic voltammograms, or their disappearance in the 'reverse' limbs on going more cathodic. The products have also been separated and analysed, and X-ray diffraction (XRD), scanning electron microscopy (SEM) and infrared (i.r.) spectroscopy have been used in order to characterize these materials.

2. Experimental details

The electrochemical and reflectance procedures for cyclic voltammetry always in 0.2 M $LiClO_4$ (at 2 mV s^{-1} for best reproducibility [1]) were exactly as in Part I [1]. Three electrochemical pretreatments of the zinc were again used: (i) -1.4 V for 60 min (ii) -1.4 V for 20 min, and (iii) -1.4 V for 20 min with aerial oxygen not removed. All potentials are cited with respect to saturated calomel electrode (SCE).

Atomic absorption spectroscopy was used to determine Zn and Fe in the products, on a Varian Techtron AA6 spectrometer, after 3 h sample digestion [3] in HCl. Phosphorus was determined as phosphomolybdate, after sample digestion to fuming in $HClO_4$, followed by addition to Na_2SO_3 solution then molybdate/hydrazine reagent, by absorbance measurement at 660 nm on a Pye–Unican u.v.–vis (series 2) spectrophotometer. Both types of measurements were checked on samples of known composition.

X-ray diffraction on powder samples was recorded on a Philips Guinier camera with Cu K_α irradiation. IR spectra were taken on a Perkin–Elmer 881 spectrophotometer.

SEM, on graphite-coated samples cut from electrodes, some frozen to -180 °C (likewise the samples from converted electrophotographic 'plates' [1]) was performed on a Cambridge Instruments 250 Mk 3 scanning electron microscope. Optical micrographs were taken on a Bausch and Lomb Lab microscope with 35 mm camera attachment.

3. Results and discussion

Hexacyanoferrate (II) with H_3PO_4 is reported [4] to confer corrosion resistance on metallic zinc, $Fe(CN)_6^{4-}$ alone inhibiting brass corrosion if at >0.005 M [5].

0021-891X

Zinc corrosion in H_2SO_3 is inhibited by hexacyanoferrate (II)/hexamethylene tetramine [6]. Both $Zn_2Fe(CN)_6$ and $K_2Zn_3[Fe(CN)_6]_2$ are precipitated from solutions of $K_4Fe(CN)_6$ + Zn salt, the latter being the less soluble, either product readily forming sols [3].

In the electrochemical anodization following three pretreatments ((i) −1.4 V for 60 min, or (ii) for 20 min, or (iii) for 20 min with oxygen from air present) with $Fe(CN)_6^{4-}$ present, with or without NaH_2PO_4, two distinct products are observed: first, a tough strongly adherent glassy layer forms, invisible because transparent when wet, but evident as white flakes on drying. At more positive potentials this glassy layer is breached, to allow sometimes copious formation of bulky gelatinous material, usually adherent, sometimes dispersing as a sol. Optical × 20 micrographs of the wet products show a *dramatic effect of NaH_2PO_4*: the gel produced by anodisation to −0.7 V is apparently the same with or without $H_2PO_4^-$; with the gel washed off, however, the glassy underlayer is crazed and broken in the absence of $H_2PO_4^-$, but whole and integral in its presence. *$H_2PO_4^-$ thus renders the glass permeable to Zn^{2+} thence gel generation*, possibly by copious water retention; SEM studies (below) are in accord.

3.1. *Cyclic voltammetry in hexacyanoferrate (II) with and without NaH_2PO_4*

The CVs with $Na_4Fe(CN)_6$ were in all cases different from those without. Following pretreatment (i), after a plateau from −1.1 to −1.0 V, CVs showed only a small anodic excursion starting at −1.00 V, with a barely evident cross-over there after reversal at −0.9 V, and a wide low cathodic plateau to follow. Reversal at −0.8 V (Fig. 1) evokes the main now ever-present cathodic feature at −1.20 V, which we ascribe to gel reduction. Minor preceding features at −1.1 and −1.15 V we ascribe to glass reduction and aquo Zn^{2+} reduction, the latter presumably surviving because it is locally in excess of the $Fe(CN)_6$-containing precipitant solution. Successive cycles to −0.7 V generate an accumulation of gel, broadening and with no crossover, always with the large gel-reduction peak at −1.2 V but the −1.1 V peak (glass reduction) now apparently absent. If the gel is dislodged, by bubbling nitrogen, cathodic features re-appear (Fig. 1(c)). Following 15 cycles to 0.7 V, then reversal at −1.0 V, a small anodic excursion is succeeded on reversal by a clear cathodic peak at −1.15 V, indicative of aquo Zn^{2+} species' survival as such under the gel.

The coincidence of the forward traces here with $Fe(CN)_6^{4-}$-free traces suggests that Zn^{II} oxide is generated as before, but reacts quite slowly (comparable with the few minutes' timescale of the scan) with the $Fe(CN)_6^{4-}$ to form the glass. This is breached at potentials positive of ~ −0.85 V to generate aquo Zn^{2+} species which themselves form gel with the hexacyanoferrate (II). (Dislodged gel disperses through the solution as a sol, possibly undergoing further changes of composition).

Following pretreatment (i), with 0.045 M NaH_2PO_4 present, the anodic onset is postponed, remarkably, to −0.95 V. The CV (to −0.8 V) shows the features of Fig. 1(a), but more strongly, and the third cycle closely resembles Fig. 1(c), again with features somewhat more pronounced. The presence of phosphate thus reinforces and hastens the action of hexacyanoferrate (II), except reaction with Zn^{II} oxide, which it retards. Hydrogen bubbles are evident in the gel.

After short (20 min) precathodising (pretreatment (ii)), the Na_2HPO_4-free system (with anodic current onset at −1.24 V), if reversed at −1.2 V shows the cathodic −1.3 V Zn^{II} oxide peak, again implying intrinsic slowness of the ZnO + hexacyanoferrate (II) reaction, while reversals at −1.0 and −0.93 V led to an almost negligible reverse peak at −1.1 V, or (respectively) a large peak there, for glass reduction; the last trace showed a forward anodic plateau beyond −1.1 V indicating incipient passivation against Zn^{2+} production, but no crossover on reversal. In NaH_2PO_4 the anodic onset is postponed to −1.09 V and the Zn^{II} oxide reduction peak is absent; CV reversal at −0.7 V again reproduces a first cycle CV resembling Fig. 1(c) but now with muted features. The enhancements and accelerations by NaH_2PO_4 are thus as before, following pretreatment (i), as is the retardation of the ZnO + ferrocyanide reaction.

Following pretreatment (iii) (−1.4 V, 20 min, aerial oxygen present), the initially present Zn^{II} oxide shows up notable features. For instance, without NaH_2PO_4, reversal at either −1.2 V or the much more anodic −0.83 V shows a reverse peak at −1.3 V indicating Zn^{II} oxide reduction, but with NaH_2PO_4 present this peak is supplanted by one at −1.1 V, thus *with pre-existing Zn^{II} oxide*, NaH_2PO_4 accelerates its reaction with hexacyanoferrate(II), in contrast with the retardation imposed on freshly (electrochemically) generated Zn^{II} oxide. However, gross irreproducibility can occur, especially when bursts of noise are imposed on the current across anodic regions (often following passivating plateaux at −1.2 and −1.15 V), probably resulting from spontaneous apparently chemical corrosion of Zn by $Fe(CN)_6^{4-}$ with hydrogen generation elsewhere on the zinc. Figure 2 (no NaH_2PO_4) shows contrasting behaviours in the same conditions, where in the reverse limbs a residual −1.15 V and −1.35 V peak contrast with but one −1.15 V peak; there are interesting passivating plateaux in the forward anodic region of the second sample.

Provided the noisy runs were discarded, however, it was instructive to consider the interplay between $Fe(CN)_6^{4-}$ and NaH_2PO_4, as in Fig. 3 where concentrations were varied. Dilution of $Na_4Fe(CN)_6$ by half has little consequence, but enhanced concentration, to 0.03 M, results in so impervious a deposit as to almost shut off all electrochemistry. Halving of NaH_2PO_4 diminishes all the features, doubling it enhances them all, so demonstrating its 'enabling' role with hexacyanoferrate (II). All these traces have an anodic passivation plateau (or peak) at ~ −1.2 V in the forward limb, and features at −1.0 V (except for

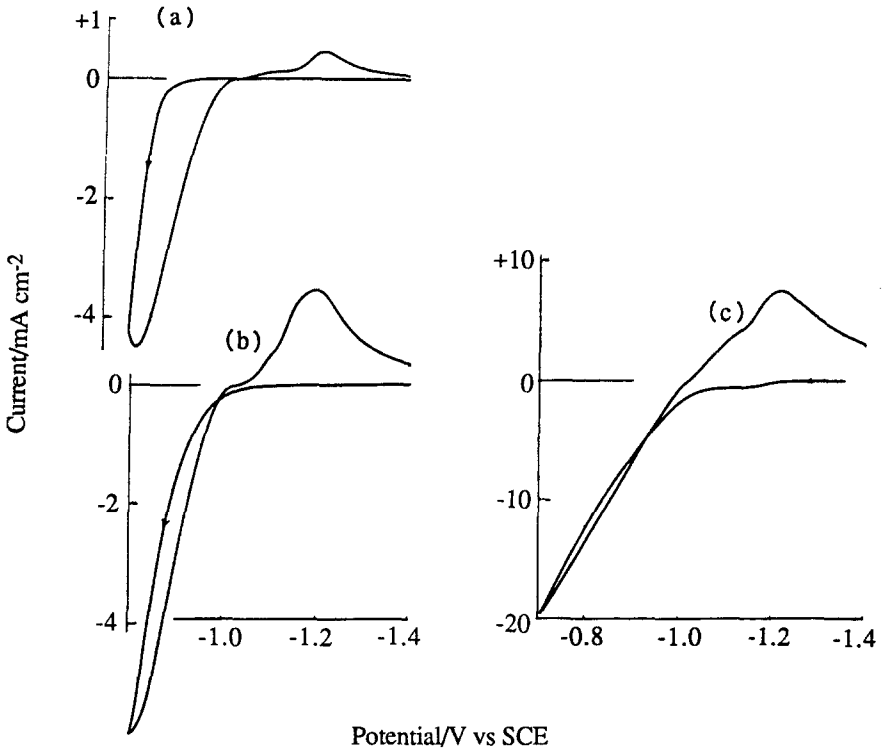

Fig. 1. (a). CV following pretreatment (i) in 0.008 M $Na_2Fe(CN)_6$, 0.2 M $LiClO_4$, pH 4.6, reversed at −0.8 V (that reversed at −0.9 V showed only an 80 μA anodic excursion). (b) Second CV following (a), also reversed at −0.8 V. (c) CV after > 15 cycles, reversed at −0.7 V, following dislodging of gel coating.

0.03 M hexacyanoferrate (II)) and −1.2 V in the reverse, with anodic crossovers on reversal resulting from the anodic-region passivations.

3.2. *Cyclic voltammetry with EDTA · Na_2 and malic acid*

Without NaH_2PO_4 following pretreatment (i), Fig. 1(a) is quite closely reproduced in 8.9×10^{-4} M EDTA; with NaH_2PO_4 the same behaviour is enhanced (i_p values ~ doubled). Pretreatment (iii), with EDTA, results in diminution of the Zn^{II} oxide reverse reduction peak at −1.3 V following small anodic excursions, or its replacement by the −1.1 V peak on larger excursions. No great difference is seen with and without NaH_2PO_4. High [EDTA] (0.003 M) leaves less adherent gel.

With 0.02 M malic acid and no NaH_2PO_4, following (i), the first cycle is standard, as Fig. 1(a), but the reverse −1.1 V peak, *which otherwise disappears*, recurs on subsequent cycles: thus the third cycle here is still like Fig. 1(a). The glassy layer is whiter and more apparent, trapping bubbles of hydrogen, then after cycling, it peels off. Malic acid thus apparently strengthens the glassy matter at the expense of the gel. NaH_2PO_4 induces little change here. After pretreatment (iii) the −1.1 V anodic peak is replaced, following anodic noise, by wide plateaux/peaks at −1.05 and −1.25 V which we leave unassigned, but with NaH_2PO_4 present the dominant −1.1 V peak, peculiarly preserved by malic acid following (i), is restored;

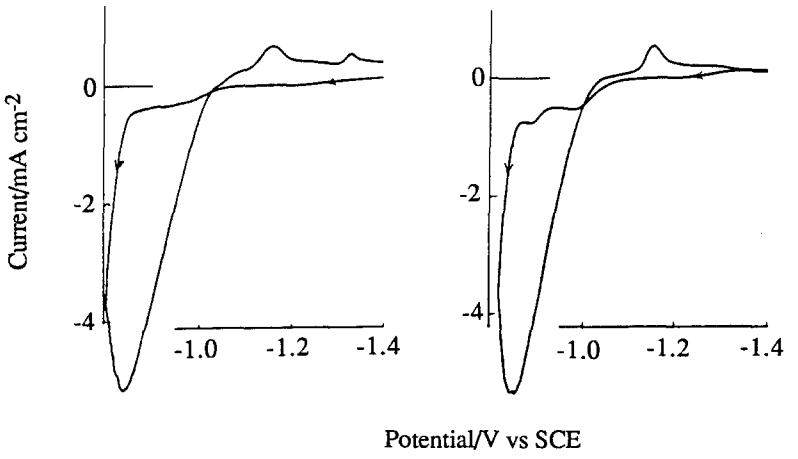

Fig. 2. First CVs, following pretreatment (iii) reversed at (left) −0.8 V and (right) −0.82 V. Note noise following reversal, and differences in anodic passivations and cathodic reductions.

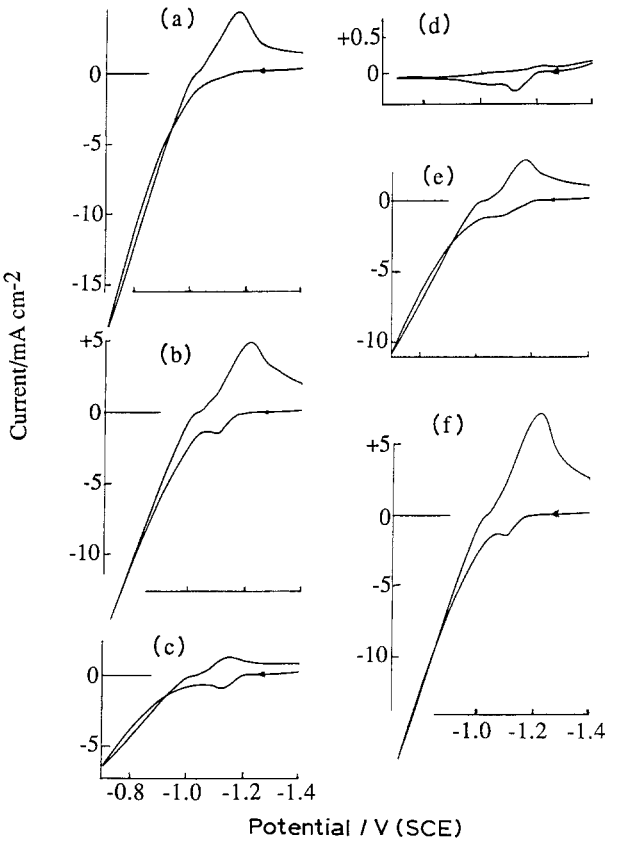

Fig. 3. First CVs following pretreatment (iii) and reversed at −0.7 V at pH 4.6, in various [$Na_4Fe(CN)_6$] and [NaH_2PO_4], respectively, as follows: (a) 0.004 M, 0.045 M; (b) 0.008 M, 0.045 M; (c) 0.016 M, 0.045 M; (d) 0.03 M; 0.045 M (e) 0.008 M 0.02 M; (f) 0.008 M, 0.09 M. Nether abscissa scales apply to CVs above.

the NaH_2PO_4-free product here appears to be intermediate between gel and glass, and in any case different from precedent: possibly Zn^{II} oxide redissolved by malic acid liberates Zn^{2+} aquo-species for reaction with hexacyanoferrate (II) in unusual environs or concentrations. Increase of malic concentration to 0.06 M weakens gel adherence.

3.3. *Cyclic voltammetry with di-sodium 1-ethoxysulphosuccinate (A102) and isopropanol (IPA)*

Following pretreatment (i), A102 at 2.5×10^{-4} M greatly diminishes the electrochemistry of Fig. 1(a), which is then more than restored on addition of NaH_2PO_4; the cathodic peaks are shifted to −1.12 and −1.22 V, respectively, owing to the insulating effects of the previously adduced strong adsorption [1,2]. After pretreatment (iii), with no NaH_2PO_4, lower currents are observed in both anodic and cathodic features, while with NaH_2PO_4 an anodic plateau sets in at −1.04 V, i.e. a less negative onset than without A102.

IPA had no detectable effect on the hexacyanoferrate (II)/Zn electrochemistry, with or without NaH_2PO_4, in contrast with the marginal effects observed in hexacyanoferrate (II)-free electrochemistry, owing no doubt to the greater robustness of the hexacyanoferrate (II) products.

3.4. *Composition and XRD*

In order to garner enough material for analyses, large ($5 \times 5\,cm^2$) electrodes were used. Glassy material was generated over 10 min from 0.06 M $Na_4Fe(CN)_6$, 0.045 M NaH_2PO_4 solution at −1.2 V. The thick adherent glassy layer was carefully scraped off (avoiding zinc flecks) and dried. (Attempted dissolution of the substrate zinc metal by HNO_3 resulted in accompanying decomposition of the required material). Gel was prepared over 5 min in 0.008 M $Na_4Fe(CN)_6$, 0.045 M NaH_2PO_4, at −0.7 V. Some samples were separated from liquid by settling over several days and decantation, others by centrifugation at 12 000 r.p.m. for 45 min.

Analyses by AAS (Table 1) of the glass (entries 1–4), the gel (entries 5–7) and a mixture of electrophotographic ZnO + commercial conversion solution (Gestetner) could possibly *all* be fitted by the formula $Zn_zX_xY_y = Zn_7[Fe(CN)_6]_3[HPO_4]_1$, where $z = 7 \pm 1$, $x = 3 \pm 0.5$ and $y = 1 \pm 0.5$, but more precision is available. Before such elaboration, the weakness of the glass to centrifuging is to be noted, Fe being thereby lost possibly as $Na_2Zn_3[Fe(CN)_6]_2$ [3], or a more zinc-deficient species, in sol or solute form; the gel also undergoes such composition change but only marginally, and the mixture from ZnO + conversion solution hardly at all.

While stoichiometric compositions need not have ensued, the entries 9–11 in the Table do conform respectively, within the analytical limits, to:

$(Zn_2Fe(CN)_6)_4Zn(H_2PO_4)_2$ for the glassy form,
$(Zn_2Fe(CN)_6)_4NaZn(HPO_4)_{1.5}$ for the gel, and
$(Zn_2Fe(CN)_6)_4ZnHPO_4$ for gross converted ZnO.

The limits are quite the widest for the last, which is best construed as a mixture of the preceding with excess $Zn_2Fe(CN)_6$ variably replacing some $ZnHPO_4$. No Na/H ratios were determined, so these are speculative.

From XRD (Table 2) the dried out materials showed, for glass, either $Zn_2Fe(CN)_6$ or $Na_2Zn_3[Fe(CN)_6]_2$ [7], while, for gel, (here garnered after multiple cycling to −0.7 V) either weak broad bands mostly corresponding with zinc metal [7], present as visible flecks, or otherwise no lines, showing its amorphousness. No ZnO is apparent but amorphous $Zn(OH_2)$ is not excluded. These observations provide some support for the composition assignments, though no phosphate structure could be found to fit unassigned lines.

3.5. *Diffuse reflectance 'R' with cyclic voltammetry in hexacyanoferrate (II)/phosphate solutions*

Use of an optical fibre to monitor reflected white light incident as a parallel beam allowed objective monitoring of electrode surface changes. These were most evident from pretreatment (iii) and at scan rate 20 mV s^{-1} where (Fig. 4) the decrease in R on ZnO formation is diminished (cf. Part 1 [1]) because of

Table 1. Compositions of hexacyanoferrate(II)-containing products

	Sample/separation	*Number of samples*	*Zn : Fe*	*Zn : PO_4*	*Fe : PO_4*
1	Glass/settling	16	2.34 ± 0.32	5.70 ± 0.57	2.09 ± 0.25
2	Glass/centrifuged*	3	5.77 ± 0.44	–	–
3	Glass/settling†	3	3.30 ± 0.07	20.1 ± 2.7	5.90 ± 0.47
4	Glass (no PO_4)/settling	3	2.17 ± 0.16	–	–
5	Gel/centrifuged	10	2.35 ± 0.21	5.48 ± 1.08	2.44 ± 0.59
6	Gel (no PO_4)/settling	2	2.15 ± 0.05	–	–
7	Gel/settling	9	1.84 ± 0.15	–	–
8	ZnO + conversion solution‡	9	2.39 ± 0.19	7.94 ± 2.91	3.48 ± 1.40
9	(cf. 1) $Zn_9X_4Y_2$§		(2.25)	(4.5)	(2.0)
10	(cf. 5) $Zn_9X_4Y_{1.5}$§		(2.25)	(6.0)	(2.67)
11	(cf. 8) Z_9X_4Y§		(2.25)	(8.65)	(3.85)

* Damage to structure from centrifuging.
† A group exceptional in all ratios.
‡ Separation immaterial.
§ X = $Fe(CN)_6$, Y = PO_4: inferred compositions.

$H_2PO_4^-$ intervention, but a sharp forward decrease occurs at −1.2 V on reaction to form glass which, being transparent, restores *R* at about −1.1 V. Gel formation beyond −1.05 V diminishes *R* again, but on the reverse, at −1.2 V where we have posited gel reduction to occur, a second increase of *R* accompanies the restoration of the reflective zinc surface. However, some of the gel escapes as sol, and the *R* trace is subsequently blurred. Thus the second CV (Fig. 4(b)), while showing a small forward feature (−1.2 to −1.0 V), has no accompanying *R* change, but the large reverse peak at about −1.2 V is shown by changes in *R* to actually be an overlapping two-material process, possibly implicating glass + gel. Obscuration of *R* by sol from dissipated gel was always a problem in later CVs.

3.6. *I.r. spectroscopy and electron micrography*

Besides a notably broadened OH stretch at ~3500 cm^{-1}, i.r. spectroscopy (Fig. 5) showed the characteristic hexacyanoferrate (II) bands (2096 cm^{-1} and 1612 cm^{-1}) and also a broad band at 1088 cm^{-1}. This is largely assignable to phosphate, but a residual band appears even with no NaH_2PO_4 present which is ascribable to perchlorate, present at 5–10% of the phosphate component. (No adjustment of the composition estimates has been made for this incorporation.) Broadening of OH bands is commonly ascribed to H-bonding. Here the glass OH band (traces a and b) is broader than the gel OH band (trace c) and it is tempting to ascribe the more rigid glass structure to a greater extent of H bonding.

SEM at 10^4 fold magnification, see Fig. 6(a), showed that dried film, from oxygen-containing $Fe(CN)_6/H_2PO_4$ solution cycled to −1.0 V, developed roughly rectangular flakes which resulted from almost linear cracking. SEM on electrophotograhic plates showed untreated ZnO particles (Fig. 6(b)) to be much smaller than the clumped aggregates of composite resulting from conversion (Fig. 6(c), taken at −180° C): bridging over the binder [1,2] is clearly evident. Furthermore, SEM (Fig. 6(d), cf. (a)) shows that phosphate-free 0.013 M $Na_4Fe(CN)_6$ solution yields a much rougher film (studied at −180° C) than is formed with 0.045 M NaH_2PO_4 present, the former peeling off the surface more readily on warming and

Table 2. XRD peaks for gel and glass, with literature [7] *values*

Sample	*d/nm*	*d/nm [7]*
Gel	0.2481	0.247*
	0.2312	0.231*
	(0.2298)	–
	0.2094	0.209*
	(0.1758)	–
	(0.1691)	–
Glass†	0.5406; 0.5379	0.544‡ {0.541}§
	0.4503; 0.449	– {0.451}§
	0.4130; 0.4113	0.413‡ {0.408}§
	0.3570; 0.3601	0.360‡ {0.364}§
	(0.3159; –)	

* Zn metal. † Two samples. ‡ $Na_2Zn_3[Fe(CN)_6]_2$. § $Zn_2[Fe(CN)_6]_2$. Values in ( ) are unassigned.

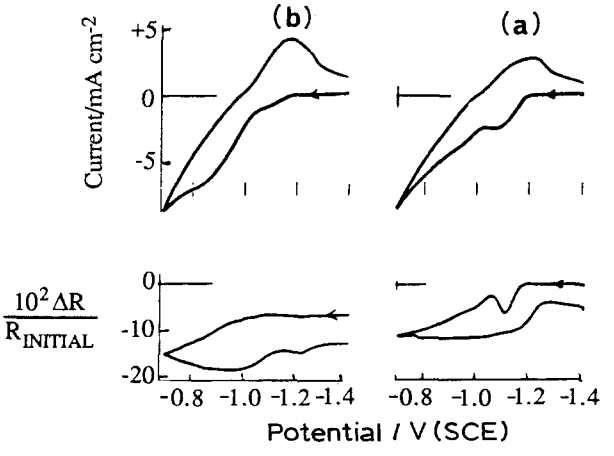

Fig. 4. CVs and percentage change in 0.013 M $Na_4Fe(CN)_6$ and 0.045 M NaH_2PO_4 at pH 4.6 following pretreatment (iii). (a) First CV, reversed at −0.7 V; (b) second CV also reversed at −0.7 V.

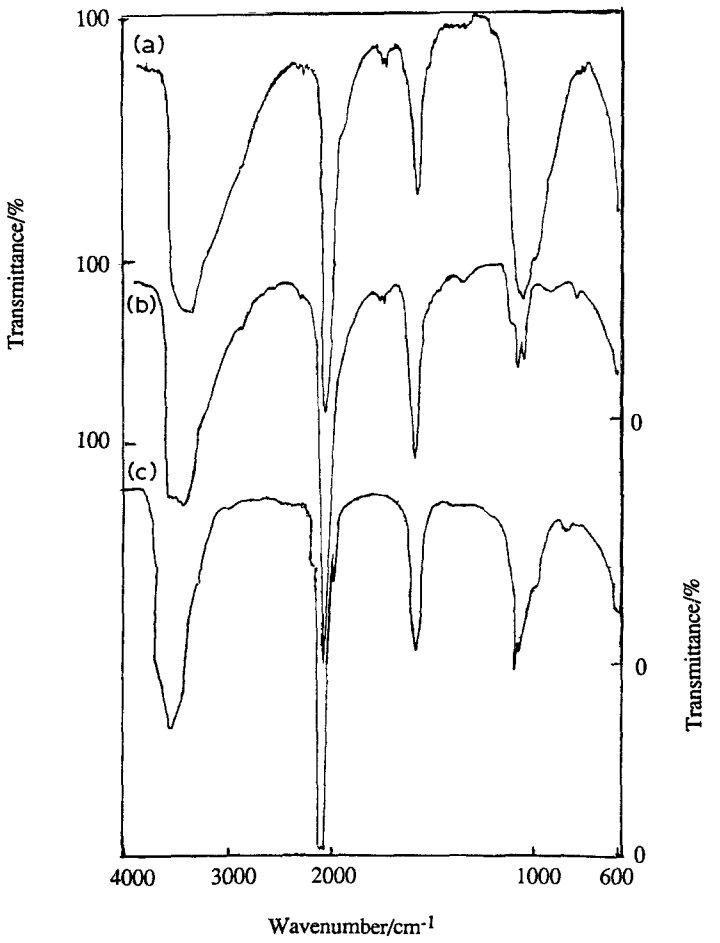

Fig. 5. I.r. spectra in KBr discs. (a) Glassy layer on zinc formed at – 1.2 V (5 min) in oxygen-containing 0.2 M $LiClO_4$, 0.06 M $Na_4Fe(CN)_6$, 0.045 M NaH_2PO_4 at pH 4.6. (b) As (a) but without $Na_4Fe(CN)_6$. (c) Gel on zinc formed at –0.7 V (5 min) in oxygen-containing 0.2 M $LiClO_4$, 0.008 M $Na_4Fe(CN)_6$, 0.045 M NaH_2PO_4, isolated by centrifuging.

drying out: retention of water on the inclusion of phosphate has been proposed [8], presumably by the H-bonding thereby introduced (a view not entirely supported by our i.r. results above which show comparable OH populations with and without phosphate). Such retention is clearly of value in inducing hydrophilicity on conversion in the electrophotographic process.

4. Conclusion

The overall picture resulting from the component-by-component study of anodically produced zinc oxide in the presence of conversion solution constituents now allows of a description of the mechanism of conversion. The hexacyanoferrate (II) forms two products comprising largely $Zn_2Fe(CN)_6$ or $Na_2Zn_3[Fe(CN)_6]_2$ with some zinc phosphate, a tough glassy material resulting from direct reaction of ZnO with hexacyanoferrate (II). Since ZnO is partly soluble at pH 4.6, Zn^{2+} aquo species are liberated to form the second gel product, which is an excellent complement to the glassy material in generating an integral hydrophilic layer over un-inked regions in the lithography. NaH_2PO_4, unusual in amplifying or depressing the electrochemical features of hexacyanoferrate (II) reactions without itself introducing dramatic processes, gives a more highly hydrated porous or permeable electrochemical glass, and in conversion will doubtless confer these properties on the product from ZnO; the consequent enhancement of hydrophilicity is especially important.

EDTA might be thought to have a deleterious effect on the conversion products (alone it weakens electrochemical Zn^{II} oxide, and in higher concentration lessens product adherence to the electrode), but its role in application may be simply the sequestering of possibly interfering cations when conversion-solution concentrates are diluted with tap water, which is often the case in practice.

Malic acid also effects a weakening of the Zn^{II} oxide, but marginally, and its role, together with NaH_2PO_4, is to buffer the pH at about 4.6, which, as noted, allows Zn^{2+} dissolution and hence gel formation.

Isopropanol is largely a humectant, to prevent plates drying out during print breaks, while the methoxysulphosuccinate, less marginally electroactive, owing to its strong adsorption on zinc, may simply play the role of surfactant wetting agent, to speed the conditioning of the lithographic plate on and after conversion.

The use of electrochemical probes thus allows the assignment of mechanistic roles to each component, and in Part IV the action of possible substitutes for hexacyanoferrate (II) will be examined by these means. Aspects of zinc electrochemistry have also been revealed which need further examination.

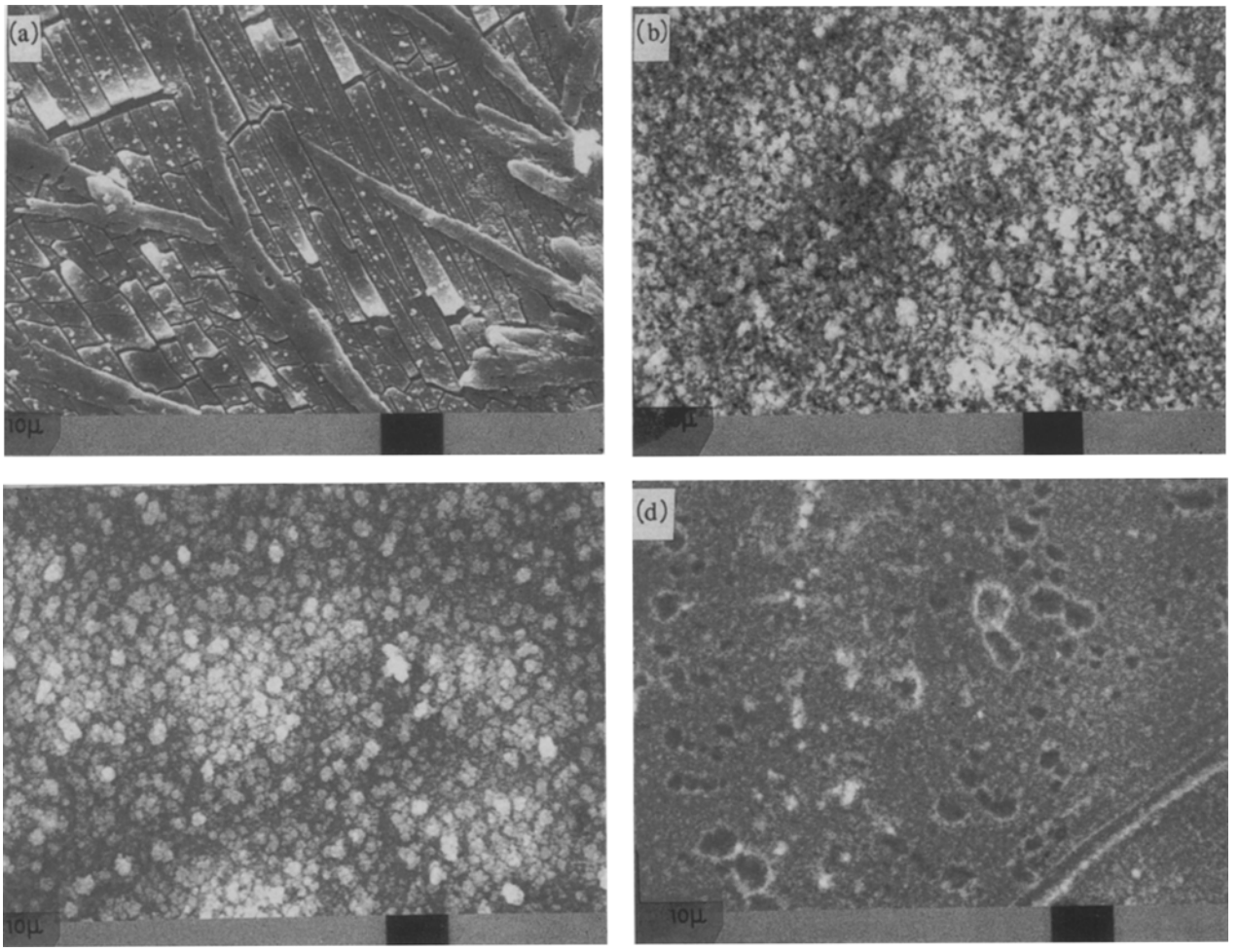

Fig. 6. SEMs $\times 10^4$. (a) Zinc electrode, cycled to -1.0 V in oxygen-containing 0.2 M $LiCLO_4$, 0.013 M $Na_4Fe(CN)_6$ and 0.045 M NaH_2PO_4, pH 4.6, 25 °C. (b) ZnO on untreated offset lithography plate. (c) As (a) but wet, cycled, electrode cooled to $-180°$ C. (d) As (c) but without NaH_2PO_4: note pits.

Acknowledgements

A.M.S. acknowledges tenure of a CASE Studentship from SERC and Gestetner Manufacture Ltd (GML), J. D. S. thanks GML for a research assistantship, and we all thank Mr D. McGee and Drs R. J. Mortimer and J. B. Jackson for assistance and advice.

References

[1] D. R. Rosseinsky, J. D. Slocombe and A. Soutar, *J. App. Electrochem.* **21** (1991) 774.
[2] D. R. Rosseinsky and A. M. Soutar, *J. Appl. Electrochem.*, **23** (1993) 187.
[3] P. A. Rock and R. E. Powell, *Inorg. Chem.* **3** (1964) 1593.
[4] K. K. Nicolskii, M. I. Gerber, O. V. Chambina, B. P. Cheneishin, I. B. Rozensvaig, *Otkajtiya Izobret. Prom. Obraztsy. Tovarnye Znaki* **49** (1972) 76.
[5] M. N. Desai and V. K. Shah, *J. Electrochem. Soc. India* **21** (1972) 98, 102.
[6] W. McLeod and R. R. Rogers, *Mater. Prot.* **8** (1969) 25.
[7] W. J. McClune, 'Powder Diffraction File, Inorganic Structures', Joint Centre for Powder Diffraction Studies (1985) p. 917.
[8] S. A. Awad and Kh. M. Kamel, *J. Electroanal. Chem.* **24** (1970) 217.